3D morphology and phase-selective transport in amphiphilic silicone hydrogels: experiments and multiscale simulations

Eri Ito[a,b], Yoshiaki Kawagoe[a], and Tomonaga Okabe[c,d,e]

[a] Research Center for Green X-Tech, Tohoku University, 6-6-11, Aoba, Aramaki, Aoba-ku, Sendai 980-8579, Japan

[b] Co-Creation Strategy Department, Menicon Co., Ltd., 3-21-19 Aoi, Naka-ku, Nagoya 460-0006, Japan

[c] Department of Aerospace Engineering, Tohoku University, 6-6-01, Aoba, Aramaki, Aoba-ku, Sendai, Miyagi 980-8579, Japan

[d] Department of Materials Science and Engineering, University of Washington, BOX 352120, Seattle, WA 98195-1750, USA

[e] Research Center for Structural Materials, Polymer Matrix Hybrid Composite Materials Group, National Institute for Materials Science, 1-2-1 Sengen, Tsukuba, Ibaraki 305-0047, Japan

All-atom MD simulation for DPD parametrization

To determine the DPD parameters, pure-component systems were individually constructed using all-atom molecular dynamics (MD) simulations, from which the density and solubility parameters were evaluated[1]. For each component, a simulation box was prepared by randomly placing 164 PDMSn5, 500 R1, 196 R2, 600 DMAA, or 200 TMSM molecules, followed by NPT equilibration at 1 atm and 300 K for 5 ns. The density and solubility parameters were obtained by averaging over the final 2.5 ns. Solubility parameters were calculated as follows:

$$\delta = \left(\frac{E_{coh}}{V}\right) = \left(\frac{-E_{nonb}}{V}\right)$$

where V is the system volume, E_{coh} is the cohesive energy, and E_{nonb} is the intermolecular potential energy, respectively. Because the total non-bonded potential energy reported by LAMMPS includes both intermolecular and intramolecular non-bonded contributions, the intermolecular potential energy was defined by subtracting the sum of all intramolecular non-bonded interactions from the total non-bonded potential energy[2]. The DREIDING-X6 force field[3] was used for the polymers, and partial atomic charges were assigned using QEq[4], [5].

Reaction model for DPD simulation

The reaction model was originally developed for all-atom MD simulations[6] and has been applied to various resin systems involving chemical reactions[7], [8], [9], [10], [11]. In our previous study, the model was extended to DPD[12], [13], where it was

demonstrated that both the crosslinking reaction and reaction-induced phase separation could be successfully reproduced.

The reaction model has two criteria, as shown in Fig. S1. The first criterion concerns the distance between the reactive beads. When the distance between the reactive beads is within the reaction cutoff ($0.5r_c$), the bead pair becomes a reaction candidate. The second criterion is the reaction probability p_{react} calculated using Eq. (8) of the Main Text. A reaction occurs when p_{react} is greater than a uniformly distributed random number between 0 and 1, and a new harmonic bond is created between the corresponding reactive beads.

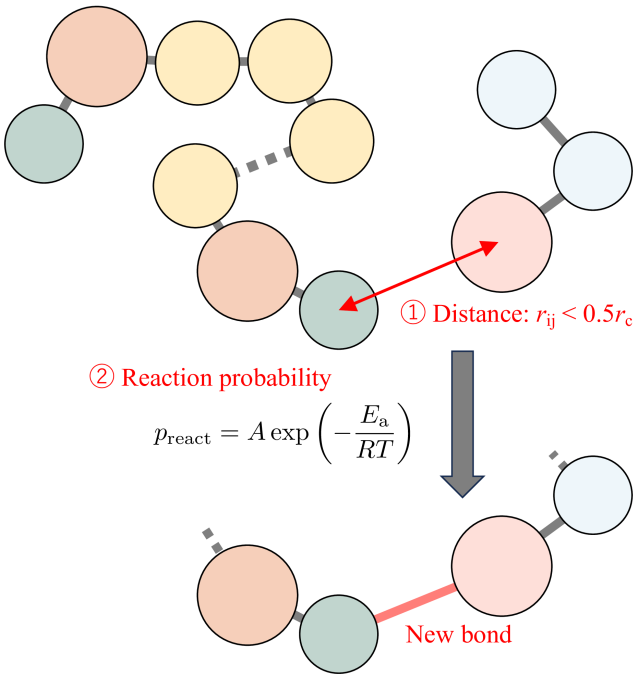

Figure S1: Polymerization diagram of the DPD simulation.

Internal Structural Imaging by TEM Observation and FFT Calculation

Two-dimensional TEM images of the binary samples 1–3 stained with ruthenium tetroxide are shown in Fig. S2. As the DMAA content increased, the staining contrast became progressively stronger, indicating an enhanced affinity of the hydrophilic domains for the staining agent. The corresponding FFT images calculated from the TEM images are shown in the upper right of each panel of Figure S2.

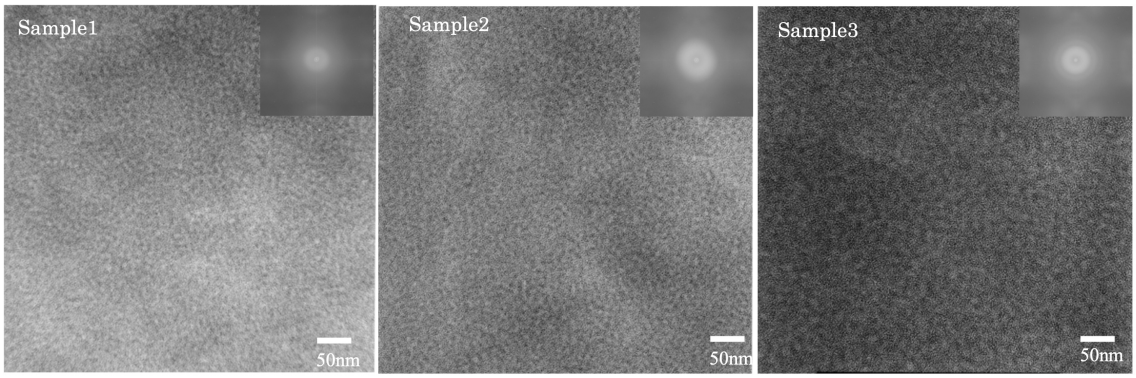

Figure S2: TEM images of samples 1–3 and the corresponding two-dimensional FFT patterns calculated from the TEM images.

For Sample 2, the TEM image previously reported by us (Ref. [14]) was used, and the FFT analysis was carried out in the same manner as for the other samples. As discussed in the Main Text, the radial profiles obtained from these FFT patterns revealed that the characteristic domain size increased with increasing DMAA content, demonstrating the systematic growth of the phase-separated structure.

Three-Dimensional Tomographic Movie Reconstructed from TEM Imaging

The supporting movies present reconstructed slice images along the x, y, and z directions as well as rotational views generated from oblique projection datasets. These videos clearly depict the three-dimensional distribution of the stained and unstained regions within the material. The reconstructed volumetric data further demonstrated that both stained and unstained domains formed distinct, continuously interconnected networks throughout the entire sample.

References

[1] K. Li, et al., “Determination of interaction parameters in a bottom-up approach employed in reactive dissipative particle dynamics simulation for thermosetting polymers,” *Soft Matter*, vol. 20, no. 23, pp. 4591–4607, 2024, doi: 10.1039/d3sm01743e.

[2] C. Li and A. Strachan, “Cohesive energy density and solubility parameter evolution during the curing of thermoset,” *Polymer*, vol. 135, pp. 162–170, 2018, doi:

10.1016/j.polymer.2017.12.002.

[3] S. L. Mayo, et al., "DREIDING: A Generic Force Field for Molecular Simulations," *Journal of Physical Chemistry*, vol. 94, no. 26, pp. 8897–8909, 1990, doi: 10.1021/j100389a010.

[4] A. K. Rappé and W. A. Goddard. III, "Charge equilibration for molecular dynamics simulations," *Journal of Physical Chemistry*, vol. 95, no. 8, pp. 3358–3363, 1991, doi: 10.1021/j100161a070.

[5] Y. Wang, et al., "Development of a Transferable ReaxFF Parameter Set for Carbon- And Silicon-Based Solid Systems," *Journal of Physical Chemistry C*, vol. 124, no. 18, pp. 10007–10015, 2020, doi: 10.1021/acs.jpcc.0c01645.

[6] T. Okabe, et al., "Curing reaction of epoxy resin composed of mixed base resin and curing agent: Experiments and molecular simulation," *Polymer*, vol. 54, no. 17, pp. 4660–4668, 2013, doi: 10.1016/j.polymer.2013.06.026.

[7] Y. Kawagoe *et al.*, "Effects of the chain length of nonaromatic epoxy resins on thermomechanical and optical properties: experiments, and ab initio and molecular dynamics simulations," *Physical Chemistry Chemical Physics*, vol. 26, no. 37, pp. 24250–24260, 2024, doi: 10.1039/d4cp02357a.

[8] Y. Kawagoe, et al., "Thermal oxidative degradation of cyanate- and amine-cured epoxy resins: Experiment and ReaxFF simulation," *Thermochim Acta*, vol. 747, p. 179949, 2025, doi: 10.1016/j.tca.2025.179949.

[9] Y. Xi *et al.*, "Enhancing epoxy resin curing: Investigating the catalytic role of water as a trace impurity in dense crosslinked network formation using an advanced cat-GRRM/MC/MD Method1," *Polymer*, vol. 313, no. September, p. 127675, 2024, doi: 10.1016/j.polymer.2024.127675.

[10] Y. Kawagoe and T. Okabe, "Evaluations of atomic-resolution strain fields using molecular dynamics simulations combined with corrected smoothed particle hydrodynamics," *Computational Material Science*, vol. 228, p. 112333, 2023, doi: 10.1016/j.commatsci.2023.112333.

[11] N. Odagiri et al., "Amine/epoxy stoichiometric ratio dependence of crosslinked structure and ductility in amine-cured epoxy thermosetting resins," *Journal of Applied Polymer Science,* vol. 138, no. 23, p. 50542, Jun. 2021, doi: 10.1002/app.50542.

[12] Y. Kawagoe, et al., "Thermoset resin curing simulation using quantum-chemical reaction path calculation and dissipative particle dynamics," *Soft Matter*, vol. 17, no. 28, pp. 6707–6717, 2021, doi: 10.1039/d1sm00600b.

[13] Y. Kawagoe, et al., "Dissipative Particle Dynamics Simulation for Reaction-

Induced Phase Separation of Thermoset/Thermoplastic Blends," *Journal of Physical Chemistry B*, vol. 128, no. 8, pp. 2018–2027, 2024, doi: 10.1021/acs.jpcb.3c07756.

[14] K. Yamamoto, et al., "Phase-separated conetwork structure induced by radical copolymerization of poly(dimethylsiloxane)-α, ω-diacrylate and N,N-dimethylacrylamide," *Macromolecules*, vol. 42, no. 24, pp. 9561–9567, 2009, doi: 10.1021/ma9009774.